Generation of linearly polarized modes using a digital micromirror device and phase optimization

N.A. Correa-Rojas [1], R.D. Gallego-Ruiz [2], M.I. Álvarez-Castaño [1]
[1] Faculty of Engineering, Department of Electronics and Telecommunications, Metropolitan Technological Institute, Medellin Calle 54A 30-01, Colombia,
[2] Faculty of Engineering, Department of Electronics and Telecommunications, University of Antioquia, A.A. 1226, Medellin, Colombia

Abstract

Linearly polarized modes were generated from the fundamental LP_{01} using Lee holograms displayed on a digital micromirror device. The phase in the holograms was optimized using simulated annealing algorithm and complex amplitude correlation to improve the quality of the converted modes. The correlation measurements, and comparisons between numerical and experimental results, show the fidelity of the obtained modes and the effectiveness of the optimization. Furthermore, the optimized holograms can be combined to generate multiple modes spatially addressed with individual control. The results, and the use of a digital micromirror device instead of the most common liquid crystal modulators, make this method suitable for Modal Division Multiplexing systems and compatible with other optical telecommunication techniques like Wavelength and Polarization Division multiplexing, and reconfigurable optical networks.

Keywords: phase modulation, spatial light modulators, diffractive optics, free-space optical communication, optical communications, modes; buffers, couplers, routers, switches, and multiplexers.

Citation: Correa-Rojas NA, Gallego-Ruiz RD, Álvarez-Castaño MI. Generation of linearly polarized modes using a digital micromirror device and phase optimization. Computer Optics 2022; 46(1): 30-38. DOI: 10.18287/2412-6179-CO-857.

Acknowledgments: The work was funded by the Metropolitan Technological Institute (Instituto Tecnológico Metropolitano), grant number P20222.

Introduction

The expected reach of the physical limits of optical communications systems based on single-mode fibers demands the exhaustive use of every degree of freedom of the light [1 – 3]. The Wavelength, time, amplitude, and state of polarization are particularly widely used as multiplexing methods but appear to be short to satisfy the demand growth trend. On the other hand, the spatial domain is taking increasing attention recently as a promising physical layer to overtake these limitations. Space Division Multiplexing (SDM) uses the space for effectively separate data channels. In this order, it has been applied with multicore fibers (MCF), free space, and multimode fibers (MMF) [4 – 7]. However, from the point of view of cost per bit, scalability, and transmission capacity, SDM in multimode fibers that can only support a small number of modes, called few-mode fibers (FMF), shows promising advantages. These advantages come from their low differential mode group delay (DMGD), extended Shannon limit, and feasibility to apply multiple-input-multiple-output (MIMO) signal processing to deal with crosstalk [8 – 14]. SDM using different modes of a single optical fiber is often called mode division multiplexing (MDM) [15].

In MDM, spatial optical modes, like Laguerre-Gauss modes (LG) or Linearly Polarized modes (LP), can be used as individual channels [2, 8, 9, 16]. MDM has been applied co-propagating modes in free-space or in optical fibers [5, 15, 17 – 24]. In both cases, is necessary to manipulate optical modes in a process called mode conversion. This process transforms an incoming mode or superposition of several modes into another mode or modes. Thus, the modal converter performs the multiplexing and demultiplexing of spatial modes [7, 22 – 25]. Despite both processes are similar, modal demultiplexing may deal with optical modes that could have been distorted during the propagation throughout the optical link, and needs signal processing or robust optical techniques like has already have been demonstrated successfully using versatile correlation filters [26, 27].

In general terms, a multi-channel optical communication system based on MDM consists of a multiplexer that generates and combines several optical modes, a transmission line or medium, and a demultiplexer that separates the modes and addresses them towards detectors. This system has been successfully proved using several approaches to mode conversion, including diffractive optical elements, mechanical actuators, integrated photonics, and spatial modulators [4, 7, 10, 16, 22 – 25, 28 – 32]. The modal converter is a key component in MDM and could be understood in a similar way as the Arrayed Waveguide Gratings (AWG) in Wavelength Division Multiplexing (WDM) [19, 24]. With a sight in reconfigu-

rable optical networks, between the several techniques that have been applied for mode conversion [5, 22 – 24, 28, 31, 33 – 42] Spatial Light Modulators (SLM) can perform arbitrary mode conversion, switching and commuting, precisely and dynamically in a controlled way [5, 28, 30, 31, 33 – 44]. However, SLMs based on Liquid Crystal (LC-SLM) would have significant limitations in optical communications systems due to their strong dependence of the phase modulation depth with the state of polarization and wavelength, low frame rate, and high scattering, among others. In this way, SLMs based on Digital Micromirror Devices (DMD) are getting increasing interest in different optical applications because of their capability to modulate phase and amplitude in a precise but straightforward manner, and generate practically any kind of laser beam, even with pulsed lasers [45 – 51].

A DMD is a reflective, binary amplitude SLM, in which the spatial distribution of its reflectance is controlled by individually changing the tilt of each micromirror in the array between two states. While LC-SLMs modulate phase as a spatially programable phase retarder, DMDs modulate phase and amplitude through a diffractive process.

DMDs are a microelectromechanical system that can achieve frame rates two orders of magnitude higher than LC-SLM. Moreover, as DMDs operate by reflection over flat micromirrors, phase modulation depth is independent of the wavelength and polarization state of light. Thus, DMDs could be implemented in reconfigurable optical networks in combination with several multiplexing methods, as MDM, WDM, and polarization-division multiplexing (PDM).

There are several methods to modulate phase and amplitude with a DMD [45]. However, binary amplitude holograms, called Lee holograms, are a simple but effective way [52, 53]. In this direction, the most notorious disadvantage of the DMD is a diffraction efficiency of only about 9 % [46, 54]. However, in many applications increasing the laser power is enough to overcome this problem. There are other very good methods for generating optical modes using binarization processes [55 – 58]. However, these methods result in phase distributions that can only be used directly in diffractive optical elements or LC-SLMs.

Optical modes in an incoming beam can be converted to other modes, or decomposed into its orthogonal components, by spatial modulation of their phases and amplitudes. This is a well-known and effective process, mainly with computer-generated spatial distributions of complex amplitudes, that has been applied using different kinds of spatial filters or modulators over several families of optical modes. [39, 43, 59 –64]. In a FMF with a step-index profile and fulfilling the weak guidance approximation, several Linearly Polarized (LP) modes propagate throughout the fiber. These modes can be converted by adding to an incoming mode its phase difference respect any other mode [64]. To convert LP modes using a DMD is needed to perform the transformation in free space. In this order, the difference in boundary conditions between the confined medium of the optical fiber and the free-space affects the conversion quality. If only the phase difference between the two modes is added to the incoming mode by the DMD, an important amount of the power of the outgoing converted mode will spread out distorting its shape. To ensure the efficient coupling of the modes back to the FMF, low intermodal crosstalk, and power efficiency in the conversion, an optimization of the conversion must be done [35, 42]. Among the several optimization methods, Simulated Annealing (SA) algorithm has proven to be suitable for phase masks optimization in similar applications [65 – 67].

In this work, we propose a mode converter based on a DMD SLM. Several LP modes were generated from the fundamental LP_{01} using Lee holograms. The phase in the holograms was optimized using SA algorithm and complex amplitude correlation to improve the quality of the converted modes. The correlation measurements, and comparisons between numerical and experimental results, show the fidelity of the obtained modes and the effectiveness of the optimization. Furthermore, the optimized holograms can be combined to generate multiple modes spatially addressed with individual control. The results and the use of a DMD instead of a LC-SLM make this method suitable for MDM systems and compatible with other optical telecommunication techniques like WDM, PDM, and reconfigurable optical networks.

1. Basic principles

The DMD is a binary amplitude SLM consisting in an addressable array of micromirrors in which each mirror can be precisely tilted between to two states, defining the ON and OFF states. In this manner, an optical field $\Psi(x, y)$ with an amplitude $A(x, y)$, phase $\phi(x, y)$, defined as equation (1)

$$\Psi(x,y) = A(x,y)\exp[i\phi(x,y)], \tag{1}$$

can be generated by displaying on the DMD the binary reflectance of a Lee hologram. This reflectance is defined as follow in equation (2) [45], as

$$H(x,y) = \frac{1}{2} + \frac{1}{2}\operatorname{sgn}[\cos[2\pi\nu_0 x + \phi(x,y)] - \cos[\pi\omega(x,y)]], \tag{2}$$

where sgn is the sign function, ν_0 is the carrier frequency in the x direction that separates the diffraction orders in the optical reconstruction, and $\omega(x,y)$ is a function related with the optical field amplitude, by

$$\omega(x,y) = \frac{1}{\pi}\arcsin[A(x,y)]. \tag{3}$$

For phase-only modulation, the amplitude is set to be uniform and unitary, so the equation (2) can be simplified as

$$H(x,y) = 1/2 + (1/2)\operatorname{sgn}[\cos[2\pi\nu_0 x + \phi(x,y)]]. \tag{4}$$

In a conventional step-index optical fiber with a core radio a, working wavelength λ, the electric field of LP weakly-guided modes, linearly polarized in the x direction, and propagating in the z direction, can be represented in cylindrical coordinates as

$$E_{ml} = \begin{cases} J_m\left(\frac{r}{a}u_{ml}\right)\cos\left[l\theta\right]e^{-i\beta z}, r \le a \\ \frac{J_m(u_{ml})}{K_m(u_{ml})}K_m\left(\frac{r}{a}w_{ml}\right)\cos\left[l\theta\right]e^{-i\beta z}, r > a. \end{cases} \quad (5)$$

Where J_m is the ordinary Bessel function of first kind and m order, K_m is the modified Bessel function of second kind and m order. The integers m and l are the radial and azimuthal indices, respectively, u_{ml} and w_{ml} are the normalized transverse constants of attenuation and phase, respectively, and β is the longitudinal propagation constant [36].

To convert an incident LP_{ml} mode into another, the phase difference between the two modes is calculated by using equation (5) and its argument, i.e., to convert an incident LP_{in} mode into a LP_{out} mode, the phase distribution to be used in the hologram calculation in equation (4) is obtained as

$$\phi(x,y) = \arg\left[LP_{\text{out}}\right] - \arg\left[LP_{\text{in}}\right]. \quad (6)$$

The phase in equation (6) would make a perfect mode conversion if the process occurred inside the boundary conditions of the optical fiber. However, in free-space the phase in (6) needs to be optimized to ensure the fidelity of the converted modes respect the analytical modes, which leads to a better power conversion and coupling efficiency, and lower intermodal crosstalk [36, 42, 66]. Thereby, taking as starting point equation (6), the phase to be displayed on the DMD is optimized by SA algorithm. SA is a metaheuristic inspired in the annealing process of solids that has been successfully applied in optimizing phase masks [65 – 67]. SA uses the Boltzmann probability distribution to randomly accept or reject changes that get a worse solution. This simple step is effective to avoid local extrema.

One important part of the optimization is the correlation function used as cost function. Usually, the comparison between the optimized and target optical field is made using intensity profiles and correlations like Pearson or Mean Square Error. However, to have a complete mode conversion, in amplitude and phase, we made the optimization comparing complex amplitudes. Thus, we use a cost or correlation function of complex values, which corresponds to a normalized dot product, defined as [68]

$$r = \left|\sum_{i=1}^{n} M_i T_i^*\right|^2 \Big/ \sum_{i=1}^{n}\left|M_i\right|^2 \sum_{i=1}^{n}\left|T_i\right|^2, \quad (7)$$

where M_i is the converted mode from the phase in the optimization, and T_i is the analytical target mode. Equation (7) is also applied to measure the similarity between modes and construct the crosstalk matrices.

The modal conversion is performed using diffractive properties of the Fourier optics in a 4f system. The phase is added to an incoming mode in a Fourier conjugate plane. The converted mode is the far-field diffraction pattern of the incoming mode with the added phase. Experimentally, the phase is coded in a Lee hologram, with a carrier to separate the diffraction orders and a spatial filter to finally take only the outgoing converted mode.

2. Results and experiments

In general terms, the modal conversion is performed using optical Fourier processing in a 4f system. fig. 1 shows the numerical results of 4 LP modes (LP_{11}, LP_{21}, LP_{31}, LP_{41}) converted from incident LP_{01} using to non-optimized phase masks. The incident LP_{01} is shown in fig. 1*a*, the phase masks in fig. 1*b* were calculated using equation (6), and the theoretical and converted modes are in fig. 1*c* and fig. 1*d*, respectively. It can be seen the effect of the conversion in free space in power distribution without the boundary conditions of the optical fiber.

To a better conversion efficiency, the previous phase masks were optimized through SA algorithm and the correlation of complex amplitudes. Fig. 2. shows the numerical modal conversion using optimized phases. The incident fundamental mode is shown in fig. 2*a*. Fig 2*b* shows the optimized phases used. Fig. 2*c* and fig. 2*d* show the target theoretical modes and the modes obtained using the phases in fig. 2*b*. Converted modes form the optimized phase masks exhibit morphological similarities to the expected modes fig. 2*d*. Qualitatively, the power distribution is closer to the analytical modes compared with the previous non-optimized modes.

Quantitative comparison through a correlation between the converted patterns from non-optimized and optimized mask and the analytical expected mode are shown in fig. 3. As expected, lower correlation values were achieved when we used the non-optimized mask, and noticeable higher values for conversion with the optimized mask, where none of the correlation values was below 0.96. Improvements up to 118 % in correlation were obtained by optmization.

Experimentally, to make a mode conversion using DMD a SLM the basic principle consists in display on the DMD a Lee hologram and project a collimated input mode over the DMD, to be converted into a desired mode. The experimental setup of the mode conversion system is shown in fig. 4. A laser beam (Thorlabs HNL100L He-Ne 632.8 nm) is focused on a step-index single-mode fiber (SMF) using a microscope objective (MO). The collimated output beam was projected toward the DMD (Texas Instruments DLP LigthCrafter 6500) used as SLM. The hologram $H(x, y)$ generated by equation (4) is displayed on DMD to generate the desired LP mode. A linear carrier was used to separate the diffraction orders, and a spatial filter takes out the first diffraction order with the converted mode. The incident mode becomes converted into the expected mode due to the 4f opti-

cal Fourier processing system formed by lenses L1 and L2. Besides, lenses L2 and L3 form another 4f system with the spatial filter (SF) for selecting the proper diffraction order with the converted mode and imaging on the camera.

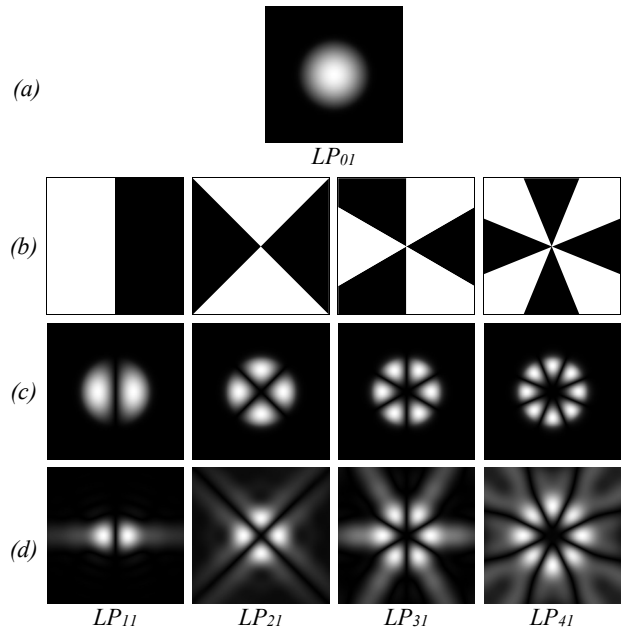

Fig. 1. Numerical results of a LP_{01} mode converted into 4 different LP modes (LP_{11}, LP_{21}, LP_{31}, LP_{41}) using non-optimized phase masks form equation (6). (a) Incident mode LP_{01}. (b) Phase masks used for converting the incident mode to expected modes. (c) Theoretical modes or expected modes. (d) Results of converted modes

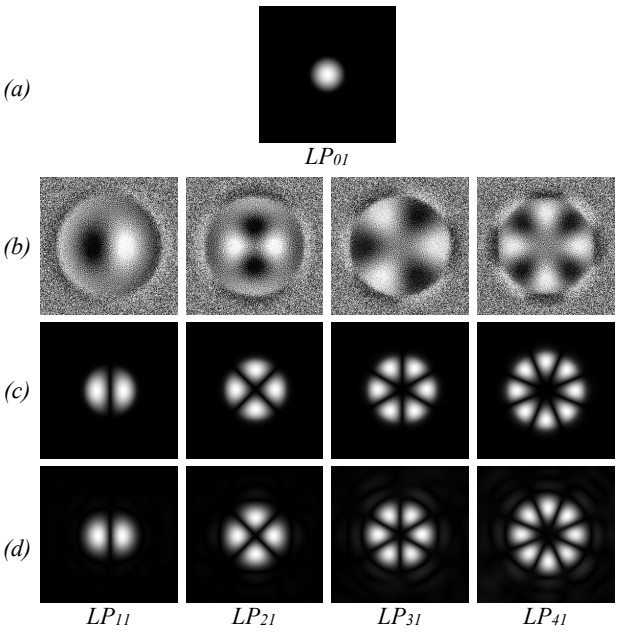

Fig. 2. Numerical results of 4 different converted modes using optimized phases.(a) Simulated incident LP_{01} mode. (b) Arrangement of Optimized phase masks by SA algorithm used for converting the incident mode to expected mode. (c) Theoretical modes or expected modes. (d) Resulting converted modes from optimized masks

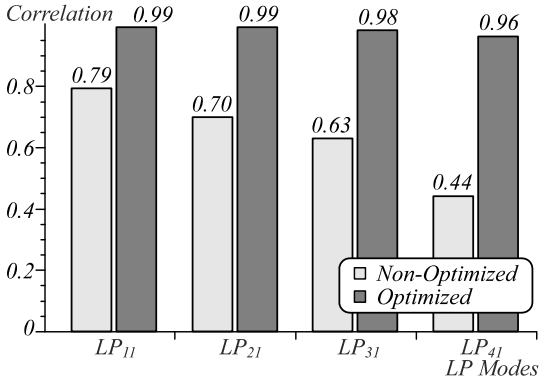

Fig. 3. Correlations comparison of numerical results for mode conversion from non-optimized phase mask, and optimized mask by SA algorithm

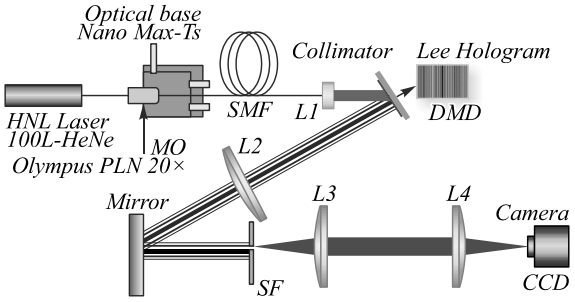

Fig. 4. Experimental setup scheme of the mode conversion system using DMD. The input mode over the DMD is modulated by using a binary amplitude hologram. Lenses L1 and L2 perform optical Fourier transform, and the spatial filter (SP) selects the first diffraction order. Lenges L3 and L4 take the outgoing converted mode to form image on the camera

For the experiment of modal conversion, we used three kind of phase masks in the form of Lee holograms. First, we generated holograms from non-optimized phases according to (6), fig. 5. Then, the optimized phases were applied in mode conversion, fig. 6. Finally, several optimized phases were used to generate multiple modes simultaneously. The space addressing of the modes were made by using a different carrier to each mode. This final procedure shows the feasibility to apply the method in an MDM system.

The experimental results of mode conversion from Lee holograms with non-optimized phases are shown in fig. 5, which were obtained by taking an input fundamental LP_{01} mode, shown in fig. 5*a*, and phases following equation (6). Fig. 5*c* and fig. 5*d* show the theoretical and the experimentally converted modes, respectively. The same expected morphological differences are found between confined modes and modes in free space.

On the other hand, noticeable better approximation to theoretical modes were obtained by using Lee holograms with optimized phases. These results are shown in fig. 6. The input mode to the optical Fourier processing system is again a fundamental LP_{01} from the SMF, shown in fig. 6*a*. The calculated Lee holograms are shown in fig. 6*b*. produced different experimental patterns of converted modes fig. 6*c* and fig. 6*d* show the theoretical and experimental converted modes, respectively. As in the numerical simulation, it can be visually seen that the optimization gives a much better approach to the target modes.

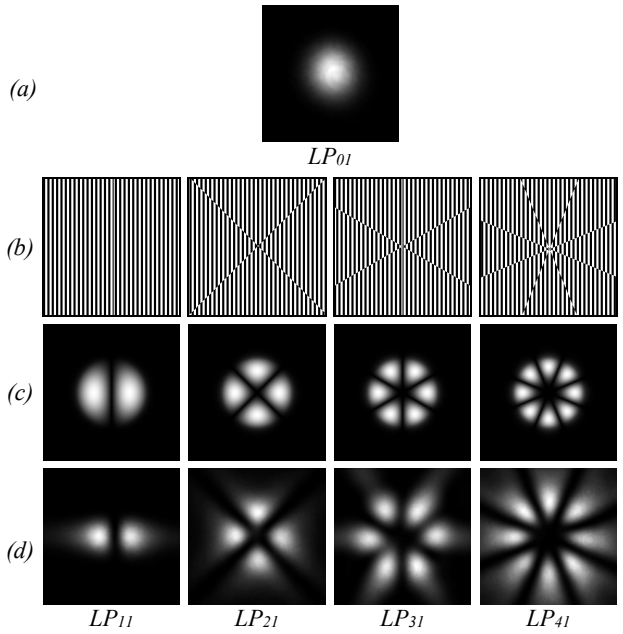

Fig. 5. Experimental results of mode conversion from non-optimized phases. (a) Experimental incident mode. (b) Binary Lee holograms with non-optimized phases. (c) Theoretical expected modes. (d) Output modes of mode conversion system produced by non-optimized phases

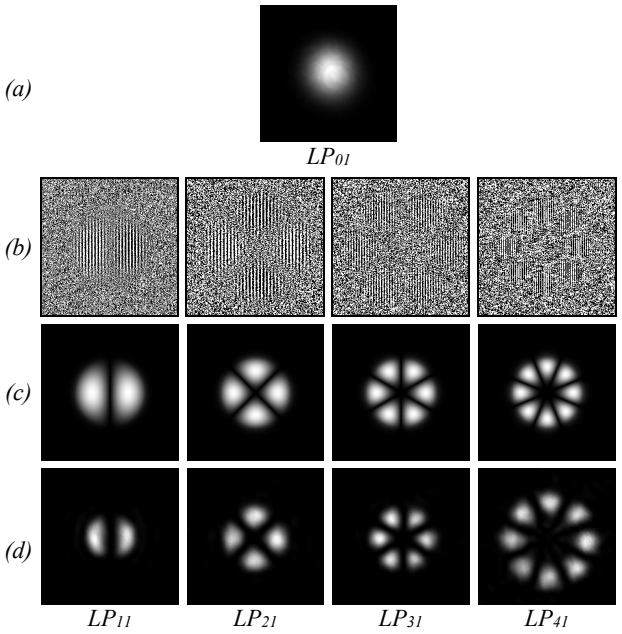

Fig. 6. Experimental results of mode conversion with optimized phases. (a) Fundamental incident mode. (b) Binary Lee holograms from optimized phases. (c) Theoretical expected modes. (d) Experimental output modes

The correlation coefficients of the converted modes (LP_{11}, LP_{21}, LP_{31}, LP_{41}), from non-optimized and optimized phases, are shown in fig. 7. There, the optimized modes have an increase in correlation up to 17 %, with maximum values of 0.94, compared with non-optimized modes The results of the multiplexed hologram are shown in fig. 11. A fundamental LP_{01} mode, fig. 11*a*, is transformed by the binary multiplexed hologram, fig. 11*b*, into four modes (LP_{11}, LP_{21}, LP_{31}, LP_{41}). fig. 11*c* and fig. 11*d* show the numerical and experimental results, respectively. Fig. 12 shows the crosstalk matrix of the four modes, with a mean value of its diagonal of 0.9.with a maximum correlation of 0.89.

Fig. 8 and fig. 9 present crosstalk matrices of experimental converted modes with non-optimized and optimized masks, respectively. The non-optimized matrix, fig. 8, has a mean in its diagonal of 0.84, while the optimized matrix, of 0.92, fig. 9.

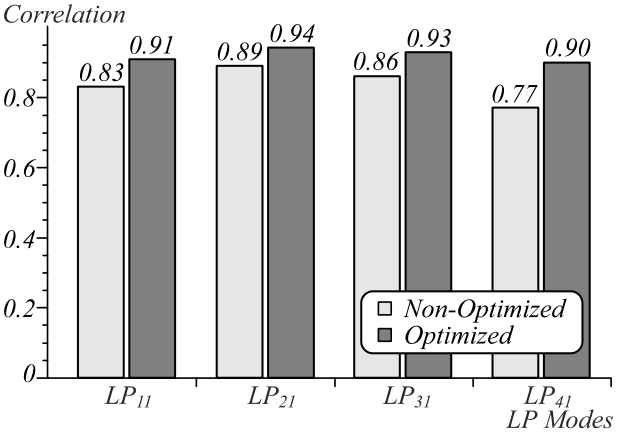

Fig. 7. Comparison of correlation coefficients of experimental mode conversion respect theoretical mode using non-optimized and optimized phases

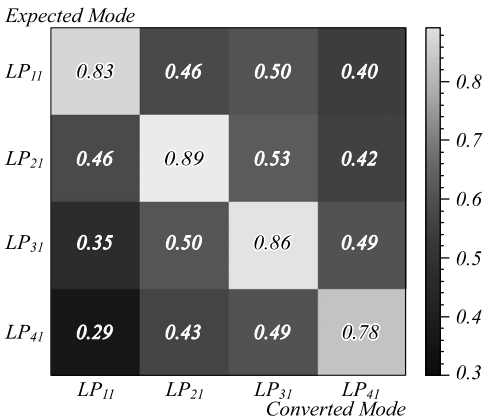

Fig. 8. Experimental Crosstalk Matrix from converted modes using non-optimized phases

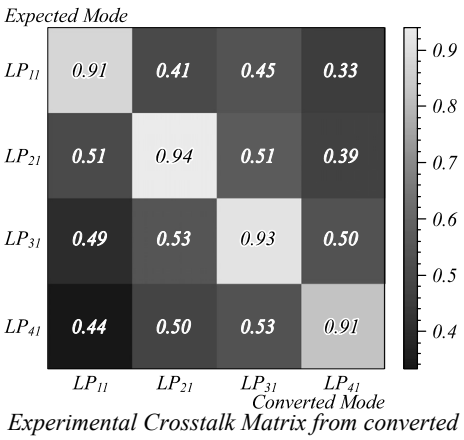

Fig. 9. Experimental Crosstalk Matrix from converted modes using optimized phases

Several modes were obtained simultaneously using the superposition of the optimized holograms. The location of each mode is easily controlled with the carrier added in the calculation of the holograms. Fig. 10 shows the schematic process to achieve a *multiplexed hologram*. The optimized phases are converted into binary Lee holograms. Each hologram has a different carrier and is finally superposed. In this case, final hologram contends all the phases needed to convert a LP_{01} mode into four different LP modes. Furthermore, using phases that make the inverse conversion, it is possible to convert several high order modes into the fundamental. This procedure shows the capability of the method to be implemented in an MDM system as multiplexer or demultiplexer.

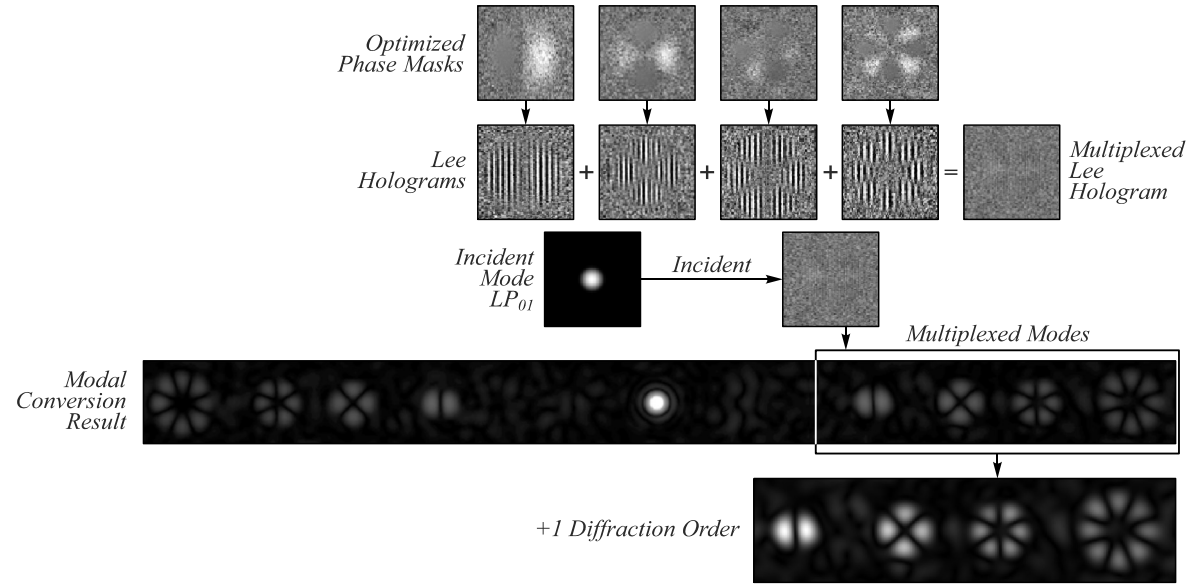

Fig. 10. Block schematic of the building process of a phase mask to create a multiplexed hologram. Holograms with optimized phases are superposed. Each hologram produces a different mode in a position determined by its carrier

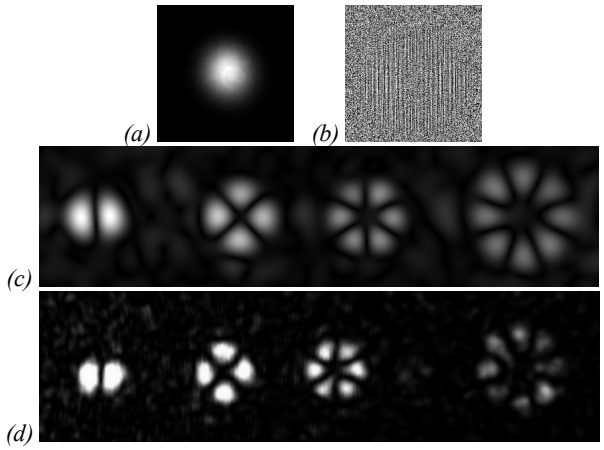

Fig. 11. Experimental results of several modes created using a multiplexed hologram with optimized phases. (a) Experimental input beam. (b) Binary Multiplexed Hologram. (c) Computational Result of multiplexed beam. (d) Experimental Results of multiplexed beam

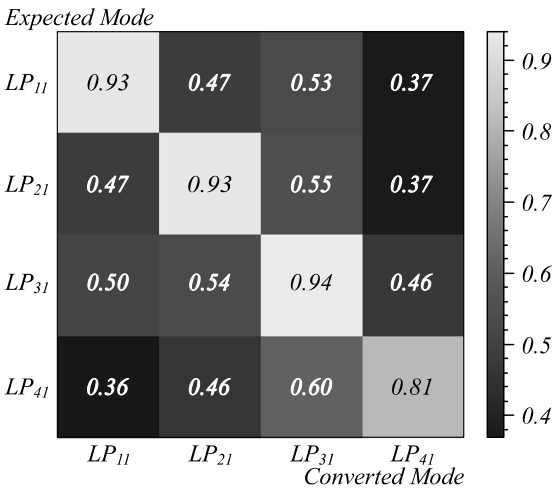

Fig. 12. Experimental Crosstalk Matrix from the multiplexed process, the diagonal has a mean valued of 0.9

Conclusions

The generation of several LP modes using a DMD as mode converter was presented. The conversions were performed using phase modulation by means of binary amplitude holograms in a Fourier optical process. Moreover, as the conversions were made in free space, the phases needed to transform the modes were optimized using the simulated annealing algorithm and a correlation function based on the complex amplitude of the optical fields. The optimization showed a noticeable improvement in the correlation of the converted modes respect the theoretical. The optimization is only needed to be done once, the phases can be then used in several ways as for multiplexing or demultiplexing modes. Crosstalk matrices showed the system is suitable for MDM architectures. The experimental results are similar with others reported that use LC-SLM, but the use of a DMD instead of a LC-SLM make this method suitable for MDM systems and compatible with other optical telecommunication tech-

niques like WDM, PDM, and reconfigurable optical networks. A quantitative comparison between expected modes and converted modes by correlation measurements shows that to achieve optimal efficiency for mode conversion it is necessary to optimize the phase mask, and the SA algorithm is suitable for the application. The presented system is controlled, reconfigurable and dynamic, could play an essential role in the massive WDM-SDM multiplexing by providing high-velocity, low-cost, flexiblility.

References

[1] Essiambre R-J, Kramer G, Winzer PJ, Foschini GJ, Goebel B. Capacity limits of optical fiber networks. J Light Technol 2010; 28(4): 662-701. DOI: 10.1109/JLT.2009.2039464.

[2] Essiambre RJ, Tkach RW. Capacity trends and limits of optical communication networks. Proc IEEE 2012; 100(5): 1035-1055. DOI: 10.1109/JPROC.2012.2182970.

[3] Ellis AD, McCarthy ME, Al Khateeb MAZ, Sorokina M, Doran NJ. Performance limits in optical communications due to fiber nonlinearity. Adv Opt Photonics 2017; 9(3): 429-503. DOI: 10.1364/AOP.9.000429.

[4] Klaus W, Puttnam BJ, Luís RS, Sakaguchi J, Delgado Mendinueta J-M, Awaji Y, Wada N. Advanced space division multiplexing technologies for optical networks. J Opt Commun Netw 2017; 9(4): C1-C11. DOI: 10.1364/JOCN.9.0000C1.

[5] Ruffato G, Massari M, Parisi G, Romanato F. Test of mode-division multiplexing and demultiplexing in free-space with diffractive transformation optics. Opt Express 2017; 25: 7859-7868. DOI: 10.1364/OE.25.007859.

[6] Essiambre R-J, Ryf R, Fontaine NK, Randel S. Breakthroughs in photonics 2012: Space-division multiplexing in multimode and multicore fibers for high-capacity optical communication. IEEE Photonics J 2013; 5(2): 0701307. DOI: 10.1109/JPHOT.2013.2253091.

[7] Weng Y, Ip E, Pan Z, Wang T. Advanced spatial-division multiplexed measurement systems propositions-from telecommunication to sensing applications: A review. Sensors (Switzerland) 2016; 16(9): 1387. DOI: 10.3390/s16091387.

[8] Li G, Bai N, Zhao N. Space-division multiplexing: the next frontier in optical communication. Adv Opt Photonics 2014; 6(4): 413-487. DOI: 10.1364/AOP.6.000413.

[9] Richardson DJ, Fini JM, Nelson LE. Space-division multiplexing in optical fibres. Nat Photonics 2013; 7: 354-362. DOI: 10.1038/nphoton.2013.94.

[10] Al Amin A, Li A, Chen S, Chen X, Gao G, Shieh W. Dual-LP_11 mode 4x4 MIMO-OFDM transmission over a two-mode fiber. Opt Express 2011; 19(17): 16672-16679. DOI: 10.1364/OE.19.016672.

[11] Winzer PJ, Foschini GJ. MIMO capacities and outage probabilities in spatially multiplexed optical transport systems. Opt Express 2011; 19(17): 16680-16696. DOI: 10.1364/OE.19.016680.

[12] Kubota H, Morioka T. Few-mode optical fiber for mode-division multiplexing. Opt Fiber Technol 2011; 17: 490-494. DOI: 10.1016/j.yofte.2011.06.011.

[13] Arik SO, Kahn JM, Ho K-P. MIMO signal processing for mode-division multiplexing: An overview of channel models and signal processing architectures. IEEE Signal Process Mag 2014; 31: 25-34. DOI: 10.1109/MSP.2013.2290804.

[14] Sillard P, Bigot-Astruc M, Molin D. Few-mode fibers for mode-division-multiplexed systems. J Light Technol 2014; 32: 2824-2829. DOI: 10.1109/JLT.2014.2312845.

[15] Berdagué S, Facq P. Mode division multiplexing in optical fibers. Appl Opt 1982; 21(11): 1950-1955. DOI: 10.1364/AO.21.001950.

[16] Willner AE, Huang H, Yan Y, et al. Optical communications using orbital angular momentum beams. Adv Opt Photonics 2015; 7(1): 66-106. DOI: 10.1364/AOP.7.000066.

[17] Wang J, Yang JY, Fazal IM, et al. Terabit free-space data transmission employing orbital angular momentum multiplexing. Nat Photonics 2012; 6: 488-496. DOI: 10.1038/nphoton.2012.138.

[18] Bozinovic N, Yue Y, Ren Y, et al. Terabit-scale orbital angular momentum mode division multiplexing in fibers. Science 2013; 340: 1545-1548. DOI: 10.1126/science.1237861.

[19] Koebele C, Salsi M, Sperti D, et al. Two mode transmission at 2×100 Gb/s, over 40 km-long prototype few-mode fiber, using LCOS-based programmable mode multiplexer and demultiplexer. Opt Express 2011; 19: 16593-16600. DOI: 10.1364/OE.19.016593.

[20] Saridis GM, Alexandropoulos D, Zervas G, Simeonidou D. Survey and evaluation of space division multiplexing: from technologies to optical networks. IEEE Commun Surv Tutorials 2015; 17: 2136-2156. DOI: 10.1109/COMST.2015.2466458.

[21] Winzer PJ. Making spatial multiplexing a reality. Nat Photonics 2014; 8: 345-348. DOI: 10.1038/nphoton.2014.58.

[22] Karpeev SV, Pavelyev VS, Soifer VA, Khonina SN, Duparre M, Luedge B, Turunen J. Transverse mode multiplexing by diffractive optical elements. Proc SPIE 2005; 5854: 163-169. DOI: 10.1117/12.634547.

[23] Soifer VA, Karpeev SV., Pavelyev VS, Duparre MR, Luedge B. Realization of an optical interconnection concept using transversal mode selection. Proc SPIE 2000; 4316: 152-162. DOI: 10.1117/12.407671.

[24] Karpeev SV, Pavelyev VS, Soifer VA, Doskolovich LL, Duparre MR, Luedge B. Mode multiplexing by diffractive optical elements in optical telecommunication. Proc SPIE 2003; 5480: 153-165. DOI: 10.1117/12.558775.

[25] Weng Y, He X, Pan Z. Space division multiplexing optical communication using few-mode fibers. Opt Fiber Technol 2017; 36: 155-180. DOI: 10.1016/j.yofte.2017.03.009.

[26] Khonina SN, Karpeev SV, Paranin VD. A technique for simultaneous detection of individual vortex states of Laguerre–Gaussian beams transmitted through an aqueous suspension of microparticles. Opt Lasers Eng 2018; 105: 68-74. DOI: 10.1016/j.optlaseng.2018.01.006.

[27] Lyubopytov VS, Tlyavlin AZ, Sultanov AK, Bagmanov VK, Khonina SN, Karpeev SV, Kazanskiy NL. Mathematical model of completely optical system for detection of mode propagation parameters in an optical fiber with few-mode operation for adaptive compensation of mode coupling. Computer Optics 2013; 37(3): 352-359. DOI: 10.18287/0134-2452-2013-37-3-352-359.

[28] Gao Y, Sun J, Chen G, Sima C. Demonstration of simultaneous mode conversion and demultiplexing for mode and wavelength division multiplexing systems based on tilted few-mode fiber Bragg gratings. Opt Express 2015; 23(8): 9959-9967. DOI: 10.1364/OE.23.009959.

[29] Wang W, Zhao J, Yu H, Yang Z, Zhang Y, Zhang Z, Guo C, Li G. Demonstration of 6×10 Gb/s MIMO-free polarization- and mode-multiplexed transmission. IEEE Photon

Technol Lett 2018; 30(15): 1372-1375. DOI: 10.1109/LPT.2018.2848226.
[30] Carpenter J, Wilkinson TD. All optical mode-multiplexing using holography and multimode fiber couplers. J Lightw Technol 2012; 30: 1978-1984. DOI: 10.1109/JLT.2012.2191586.
[31] Garcia-Rodriguez D, Corral JL, Llorente R. Mode conversion for mode division multiplexing at 850 nm in standard SMF. IEEE Photon Technol Lett 2017; 29: 929-932. DOI: 10.1109/LPT.2017.2694605.
[32] von Hoyningen-Huene J, Ryf R, Winzer P. LCoS-based mode shaper for few-mode fiber. Opt Express 2013; 21: 18097-18110. DOI: 10.1364/OE.21.018097.
[33] Lee YS, Lim KS, Islam MR, Lai MH, Ahmad H. Dynamic LP01-LP11 mode conversion by a tilted binary phase plate. J Lightw Technol 2017; 35: 3597-3603. DOI: 10.1109/JLT.2016.2599179.
[34] Labroille G, Denolle B, Jian P, Morizur JF, Genevaux P, Treps N. Efficient and mode selective spatial mode multiplexer based on multi-plane light conversion. 2014 IEEE Photon Conf (IPC 2014) 2014: 518-519. DOI: 10.1109/IPCon.2014.6995478.
[35] Igarashi K, Souma D, Tsuritani T, Morita I. Performance evaluation of selective mode conversion based on phase plates for a 10-mode fiber. Opt Express 2014; 22(17): 20881-20893. DOI: 10.1364/OE.22.020881.
[36] Mohammed W. Selective excitation of the LP11 mode in step index fiber using a phase mask. Opt Eng 2006; 45: 074602. DOI: 10.1117/1.2219425.
[37] Li S, Mo Q, Hu X, Du C, Wang J. Controllable all-fiber orbital angular momentum mode converter. Opt Lett 2015; 40: 4376-4379. DOI: 10.1364/OL.40.004376.
[38] Fernandes GM, Muga NJ, Pinto AN. Tunable mode conversion using acoustic waves in optical microwires. J Lightw Technol 2014; 32: 3257-3265. DOI: 10.1109/JLT.2014.2330955.
[39] Shwartz S, Golub M, Ruschin S. Diffractive optical elements for mode-division multiplexing of temporal signals with the aid of Laguerre–Gaussian modes. Appl Opt 2013; 52(12): 2659-2669. DOI: 10.1364/AO.52.002659.
[40] Zhao Y, Liu Y, Wen J, Wang T. Mode converter based on the long period fiber gratings written in two mode fiber. 2015 Opto-Electronics Commun Conf (OECC 2015) 2015: 1-3. DOI: 10.1109/OECC.2015.7340080.
[41] Tulikumwenayo A. Construction of multi-mode fiber modes using phase masks. Thesis Rochester Inst Technol 2013. Source: ⟨https://scholarworks.rit.edu/cgi/viewcontent.cgi?referer=&httpsredir=1&article=1026&context=theses⟩.
[42] Ferreira F, Borne D Van Den, Silva H, Monteiro P. Crosstalk optimization of phase masks for mode multiplexing in few mode fibers. OSA Technical Digest 2012: JW2A.37. DOI: 10.1364/NFOEC.2012.JW2A.37.
[43] Flamm D, Naidoo D, Schulze C, Forbes A, Duparré M. Mode analysis with a spatial light modulator as a correlation filter. Opt Lett 2012; 37(13): 2478-2480. DOI: 10.1364/OL.37.002478.
[44] Forbes A, Dudley A, McLaren M. Creation and detection of optical modes with spatial light modulators. Adv Opt Photonics 2016; 8(2): 200-227. DOI: 10.1364/AOP.8.000200.
[45] Ren Y-X, Lu R-D, Gong L. Tailoring light with a digital micromirror device. Ann Phys 2015; 527: 447-470. DOI: 10.1002/andp.201500111.
[46] Turtaev S, Leite IT, Mitchell KJ, Padgett MJ, Phillips DB, Čižmár T. Comparison of nematic liquid-crystal and DMD based spatial light modulation in complex photonics. Opt Express 2017; 25(24): 29874-29884. DOI: 10.1364/OE.25.029874.
[47] Lerner V, Shwa D, Drori Y, Katz N. Shaping Laguerre–Gaussian laser modes with binary gratings using a digital micromirror device. Opt Lett 2012; 37(23): 4826-4828. DOI: 10.1364/OL.37.004826.
[48] Zhao Q, Gong L, Li Y-M. Shaping diffraction-free Lommel beams with digital binary amplitude masks. Appl Opt 2015; 54: 7553-7558. DOI:10.1364/AO.54.007553.
[49] Cheng J, Gu C, Zhang D, Chen S-C. High-speed femtosecond laser beam shaping based on binary holography using a digital micromirror device. Opt Lett 2015; 40: 4875-4878. DOI: 10.1364/OL.40.004875.
[50] Ren Y-X, Li M, Huang K, Wu J-G, Gao H-F, Wang Z-Q, Li Y-M. Experimental generation of Laguerre-Gaussian beam using digital micromirror device. Appl Opt 2010; 49(10): 1838-1844. DOI: 10.1364/AO.49.001838.
[51] Ren YX, Fang ZX, Gong L, Huang K, Chen Y, Lu R-D. Dynamic generation of Ince-Gaussian modes with a digital micromirror device. J Appl Phys 2015; 117(13): 133106. DOI: 10.1063/1.4915478.
[52] Lee W-H. High efficiency multiple beam gratings. Appl Opt 1979; 18(13): 2152-2158. DOI: 10.1364/AO.18.002152.
[53] Davis JA, Valadéz KO, Cottrell DM. Encoding amplitude and phase information onto a binary phase-only spatial light modulator. Appl Opt 2003; 42(11): 2003-2008. DOI: 10.1364/AO.42.002003.
[54] Blanche P-A, Carothers D, Wissinger J, Peyghambarian N. Digital micromirror device as a diffractive reconfigurable optical switch for telecommunication. Journal of Micro/Nanolithography, MEMS, and MOEMS 2013; 13(1): 011104. DOI: 10.1117/1.JMM.13.1.011104.
[55] Khonina SN, Kotlyar VV, Soifer VA. Techniques for encoding composite diffractive optical elements. Proc SPIE 2003; 5036: 493-498. DOI: 10.1117/12.498521.
[56] Khonina SN, Ustinov AV. Binary multi-order diffraction optical elements with variable fill factor for the formation and detection of optical vortices of arbitrary order. Appl Opt 2019; 58(30): 8227-8236. DOI: 10.1364/AO.58.008227.
[57] Khonina SN, Balalayev SA, Skidanov RV, Kotlyar VV, Päivänranta B, Turunen J. Encoded binary diffractive element to form hyper-geometric laser beams. J Opt A–Pure Appl Opt 2009; 11(6): 065702. DOI: 10.1088/1464-4258/11/6/065702.
[58] Kotlyar VV, Khonina SN, Melekhin AS, Soifer VA. Encoding of diffractive optical elements by local phase jump method. Computer Optics 1999: 19: 54-64.
[59] Golub MA, Karpeev SV, Krivoshlykov SG, Prokhorov AM, Sisakyan IN, Soĭfer VA. Spatial filter investigation of the distribution of power between transverse modes in a fiber waveguide. Sov J Quantum Electron 1984; 14: 1255-1256. DOI: 10.1070/qe1984v014n09abeh006201.
[60] Golub MA, Karpeev SV, Kazanskiĭ NL, Mirzov AV, Sisakyan IN, Soĭfer VA, Uvarov GV. Spatial phase filters matched to transverse modes. Sov J Quantum Electron 1988; 18(3): 392-393. DOI: 10.1070/qe1988v018n03abeh011528.
[61] Bartelt HO, Lohmann AW, Freude W, Grau GK. Mode analysis of optical fibres using computer-generated matched filters. Electron Lett 1983; 19: 247-249. DOI: 10.1049/el:19830170.
[62] Kaiser T, Flamm D, Schröter S, Duparré M. Complete modal decomposition for optical fibers using CGH-based correlation filters. Opt Express 2009; 17(11): 9347-9356. DOI: 10.1364/OE.17.009347.

[63] Kaiser T, Lüdge B, Schröter S, Kauffmann D, Duparré M. Detection of mode conversion effects in passive LMA fibres by means of optical correlation analysis. Proc SPIE 2008; 6998: 69980J. DOI: 10.1117/12.783100.
[64] Gavrilov AV, Karpeev SV, Kazanskiy NL, Pavelyev VS, Duparré M, Luedge B, Schroeter S. Selective excitation of step-index fiber modes. Proc SPIE 2007; 6605: 660508. DOI: 10.1117/12.728461.
[65] Fang L, Zuo H, Pang L, Yang Z, Zhang X, Zhu J. Image reconstruction through thin scattering media by simulated annealing algorithm. Opt Lasers Eng 2018; 106: 105-110. DOI: 10.1016/j.optlaseng.2018.02.020.
[66] Gallego-Ruiz RD, Álvarez-Castão MI, Herrera-Ramírez JA, Correa NA. Optimization of phase masks using simulated annealing algorithm for mode conversion. J Phys Conf Ser 2020; 1547: 012007. DOI: 10.1088/1742-6596/1547/1/012007.
[67] Lan M, Gao L, Yu S, Nie S, Cai S, Qi X, Du Z, Ma C, Gu W. An arbitrary mode converter with high precision for mode division multiplexing in optical fibers. J Mod Opt 2015; 62(5): 348-352. DOI: 10.1080/09500340.2014.982223.
[68] Carpenter J, Wilkinson TD. Graphics processing unit–accelerated holography by simulated annealing. Opt Eng 2010; 49(9): 095801. DOI: 10.1117/1.3484950.

Authors' information

Nelson Alonso Correa-Rojas, (b. 1983) graduated from National University of Colombia – Medellin Branch. Works as teacher and researcher at the Metropolitan Technological Institute. Research interests: optical tweezers, photonics, optical communications, spatial light modulation, optical metrology. E-mail: *nelsoncorrea@itm.edu.co* .

Roobert David Gallego-Ruiz, (b. 1986), studied at the University of Antioquia. Works as technical computer consultant. Research interests: optical communications, scientific programming, photonics.
E-mail: *roobert.gallego@udea.edu.co* .

María Isabel Álvarez-Castaño (b. 1984), graduated from National University of Colombia – Medellin Branch. Works as teacher and researcher at the Metropolitan Technological Institute. Research interests: electromagnetic fields, optical tweezers, photonics, optical communications, spatial light modulation.
E-mail: *mariaalvarez7451@correo.itm.edu.co* .

Received December 28, 2020. The final version – July 6, 2021.